

Simple diagnostic technique of a single IGBT open-circuit faults for a SVM-VSI vector controlled induction motor drive

T. ORLOWSKA-KOWALSKA* and P. SOBANSKI

Department of Electrical Machines, Drives and Measurements, Wrocław University of Technology,
27 Wybrzeże Wyspiańskiego St., 50-370 Wrocław, Poland

Abstract. In this paper a simple diagnostic system for a single IGBT open-circuit faults for a two level voltage inverter-fed field oriented controlled induction motor drive was presented. A fault diagnostic procedure is carried out by utilizing an analysis of a stator current vector trajectory in α - β coordinates. An extraction of the failure information is based on monitoring of an angle between the stator current space vector and the α axis. Thanks to a diagnostic signal normalization, high robustness to false diagnosis alarms is guaranteed. To confirm the proposed method, simulation results under a wide range working condition of the induction motor drive were presented.

Key words: induction motor, voltage inverter, IGBTs, fault diagnosis.

1. Introduction

Nowadays failures of the converter-fed electric motor drives constitute an actual problem. As the faults consequence, a quality of the whole industrial processes is decreased therefore in many cases it is necessary to interrupt a work of the electric drives for their repair time duration. Unplanned drive stops could lead to high financial losses, so since many years various monitoring systems, which allow an automatic failures localization have been developed and wide applied in an industry [1, 2]. Among various kinds of faults, power converter faults, related to semiconductor or control circuit damages, are the most frequent and are estimated up to 60% of the power devices failures [3]. Thus recently quite a lot different fault detection and localization methods and techniques have been reported in technical literature.

In papers [4–12] open-switch fault diagnostic methods based on the analysis of the current vector hodograph function in the α - β complex plane were presented. In case of the first technique [4], a failure detection and a localization is achieved if an absolute value of the current vector exceeds some threshold at the time, when it takes characteristic position in the α - β coordinate system. According to a diagnostic technique introduced in [5], localization of a faulty inverter phase is realized by an analysis of the current vector hodograph also, but a faulty switch can be recognized thanks to the knowledge of phase currents polarity. In the papers [6, 7], an expansion of the previously described diagnostic methods was presented. Another approach for the open-switch fault diagnosis is based on measurements of the stator current data with clustering and the simple pre-processing algorithms [8, 9]. An identification of the data cluster which indicates the IGBT switch failure is achieved by utilizing uncomplicated calculations [8] or on the contrary, more sophisticated techniques

like artificial intelligence methods [9]. Similar methods consist in the centroid calculation of the current vector trajectory in the α - β coordinate system [10, 11] or in an a - b - c phase system [12]. For increasing the robustness to false diagnosis alarms under wide range load condition, a fuzzy logic based approach can be applied [11].

In this paper an implementation of a simple open-switch fault diagnostic method for two level voltage inverter-fed field-oriented-controlled induction motor drive was proposed. Extraction of the transistors faults symptoms is only based on tracking the angle between the stator current space vector and the α axis of the complex α - β coordinate system and the motor speed measurement. In comparison to previously described stator current-based diagnostic methods [4, 5], in the proposed technique a new failure localization procedure was carried on.

The considered fault diagnosis method is dedicated to fault-tolerant electric motor drive systems (FTEMDS) that require to identify a faulty transistor in order to perform a remedial action which ensures an uninterrupted motor drive maintenance [13]. In most cases, an essence of the FTEMDS concept is to utilize a redundant power converter, which topology allows to swap a faulty switch out with a redundant transistor or a power module. A survey of fault-tolerant inverter schemes was presented in paper [14].

2. Description of the open-switch fault diagnostic method

The basic scheme of the two-level voltage source inverter topology, which faults are considered in this paper, is shown in Fig. 1.

Figure 2 shows the ideal shapes of the stator current vector hodographs under different faulty modes of this inverter [6].

*e-mail: teresa.orlowska-kowalska@pwr.edu.pl

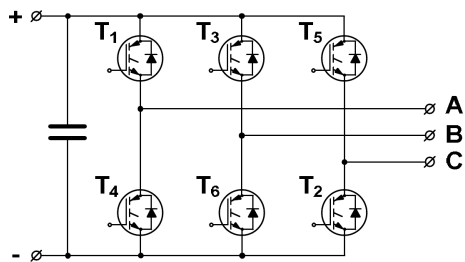


Fig. 1. Standard three-phase voltage source inverter topology

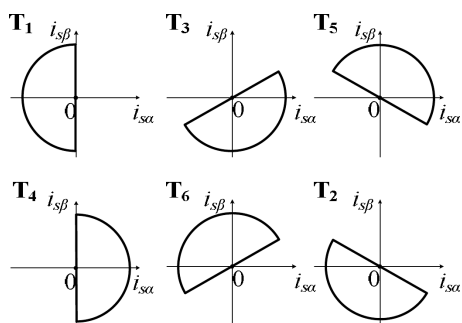


Fig. 2. Ideal shapes of the space current vector hodographs in α - β coordinate system under switch T_1 - T_6 faulty mode

As previously mentioned, the extraction of the transistor faults symptoms can be realized only by tracking the angle between the stator current space vector and the α axis of the complex α - β coordinates:

$$\Theta = \arctan\left(\frac{i_{s\beta}}{i_{s\alpha}}\right), \quad (1)$$

where $i_{s\alpha, \beta}$ are the stator currents calculated according to the Park's vector transformation (2):

$$\begin{bmatrix} i_{s\alpha} \\ i_{s\beta} \end{bmatrix} = \frac{2}{3} \begin{bmatrix} 1 & -\frac{1}{2} & -\frac{1}{2} \\ \frac{\sqrt{3}}{2} & \sqrt{3} & 0 \end{bmatrix} \begin{bmatrix} i_{sA} \\ i_{sB} \\ i_{sC} \end{bmatrix}. \quad (2)$$

Figures 3 and 4 present ideal transients of the angle, Θ , during the open-switch faults of the inverter, depending on the angular motor speed direction.

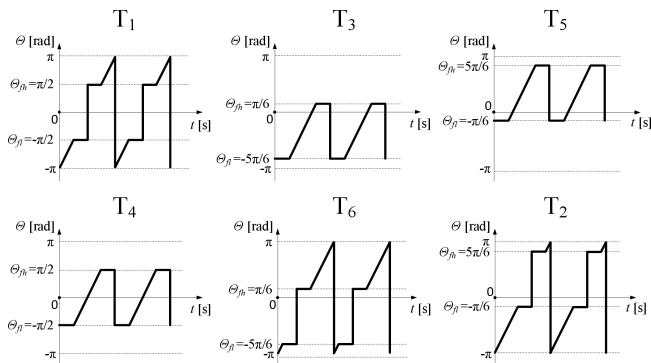


Fig. 3. The ideal transients of the angle, Θ , corresponding to faults of the transistors T_1 - T_6 under drive condition with the motor speed direction assumed as positive

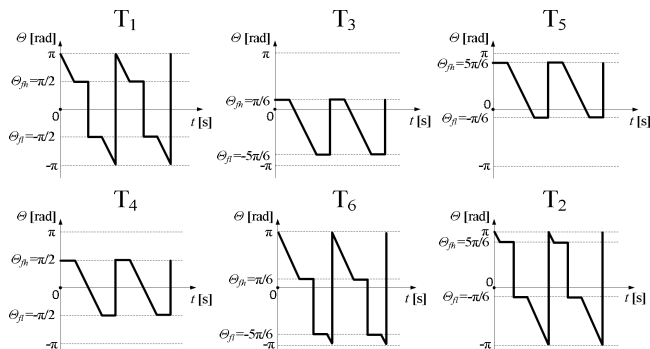


Fig. 4. The ideal transients of the angle, Θ , corresponding to faults of the transistors T_1 - T_6 under drive condition with the motor speed direction assumed as negative

When analyzing the inverter failures, one directional current in the faulty phase is observed. The situation when the current does not flow through the inverter phase, can be recognized by an analysis of some characteristic parts of the current vector hodographs. These special areas are expressed using angle Θ and are presented in Table 1.

Table 1
Characteristic parts of the current space vector hodographs carrying information about failure of the inverter phase

Faulty inverter phase	Faulty switch	Special area of hodograph expressed by using Θ [rad]
A	T_1	$\langle 0, \pi/2 \rangle$ or $\langle 3\pi/2, 2\pi \rangle$
	T_4	$\langle \pi/2, 3\pi/2 \rangle$
B	T_3	$\langle \pi/6, 7\pi/6 \rangle$
	T_6	$\langle 0, \pi/6 \rangle$ or $\langle 7\pi/6, 2\pi \rangle$
C	T_5	$\langle 5\pi/6, 11\pi/6 \rangle$
	T_2	$\langle 0, 5\pi/6 \rangle$ or $\langle 11\pi/6, 2\pi \rangle$

In case of considering failures, the stator current vector interrupts its rotating movement on the complex α - β plane two times during one period, for about quarter of a period. Position of the current vector when it is stopped, can be described by the angle Θ , and is dependent on the fault localization. These characteristic positions are presented in the Table 2.

Table 2
The characteristic positions of the stator current vector when it interrupts its rotating movement because of the switch fault

Faulty phase	Faulty switch	Characteristic positions of the stator current vector defined by Θ
A	T_1, T_4	$\pi/2$ or $-\pi/2$
B	T_3, T_6	$\pi/6$ or $-5\pi/6$
C	T_5, T_2	$5\pi/6$ or $-\pi/6$

The faulty phase is localized if the rotating current vector stops and takes a characteristic position in the α - β plane for the time t_{d1} greater than under healthy inverter mode. The faulty switch localization is achieved only by analysis of the Θ angle dynamics during the time t_{d2} between current vector stoppage. In Fig. 5, the typical parts of the Θ transients during the inverter open-switch faults were marked, as numbers 1-12.

Simple diagnostic technique of a single IGBT open-circuit faults for a SVM-VSI vector controlled induction motor drive

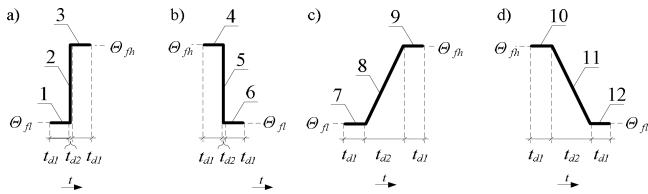


Fig. 5. The typical parts of the angle Θ transients for the inverter open-switch fault: a) sequence 1, b) sequence 2, c) sequence 3, d) sequence 4

Table 3
The open-switch fault symptoms patterns

Faulty transistor	Motor drive speed ω	Sequence of the Θ transient, which indicates the transistor fault	Characteristic positions of the stopped stator current vector defined by Θ	
			Θ_{fl}	Θ_{fh}
T ₁	$\omega > 0$	Sequence 1	$-\pi/2$	$\pi/2$
	$\omega < 0$	Sequence 2		
T ₂	$\omega > 0$	Sequence 1	$-\pi/6$	$5\pi/6$
	$\omega < 0$	Sequence 2		
T ₃	$\omega > 0$	Sequence 3	$-5\pi/6$	$\pi/6$
		Sequence 2		
	$\omega < 0$	Sequence 4		
		Sequence 1		
T ₄	$\omega > 0$	Sequence 3	$-\pi/2$	$\pi/2$
		Sequence 2		
	$\omega < 0$	Sequence 4		
		Sequence 1		
T ₅	$\omega > 0$	Sequence 3	$-\pi/6$	$5\pi/6$
		Sequence 2		
	$\omega < 0$	Sequence 4		
		Sequence 1		
T ₆	$\omega > 0$	Sequence 1	$-5\pi/6$	$\pi/6$
	$\omega < 0$	Sequence 2		

According to the assumed numbering of Θ angle transients and analysis of Fig. 3 and Fig. 4, indicated in the Fig. 5, the Table 3 was drawn up.

3. Implementation of the proposed method

Based on the observations summarized in Tables 1–3, the simple algorithm of the open-switch fault diagnosis and localization was proposed. The overall block diagram of this diagnostic system is shown in Fig. 6.

The first stage of the failure symptoms extraction procedure consists in the reduction of the Θ signal dynamics, by utilizing a low pass filter, which eliminates the high frequency diagnostic signal components. Next, in the block “FUNCTION 1” a derivative of the Θ signal is calculated, named $\Delta\Theta$, according to the equation:

$$\Delta\Theta(k) = \Theta(k) - \Theta(k - n), \quad (3)$$

where n – a number of delay time units relative to k instant.

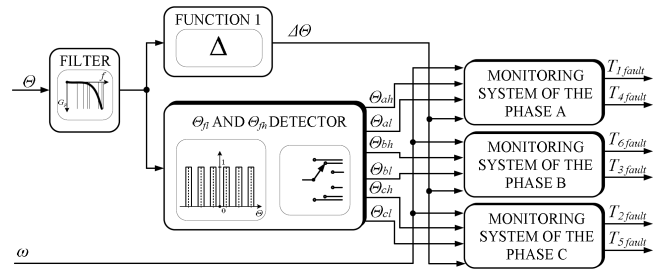


Fig. 6. Block diagram of the open switch fault diagnostic system

Simultaneously, in every simulation step, a value of the Θ signal is compared to previously defined characteristic values Θ_{fl} or Θ_{fh} . The functionality of the block “ Θ_{fl} and Θ_{fh} DETECTOR” can be explained by the following example taken for the phase A:

$$\begin{aligned} \text{if } \Theta(k) = -\pi/2 \pm \varepsilon \text{ then } \Theta_{al}(k) &= 1, \\ &\text{else } \Theta_{al}(k) = 0, \\ \text{if } \Theta(k) = \pi/2 \pm \varepsilon \text{ then } \Theta_{ah}(k) &= 1, \\ &\text{else } \Theta_{ah}(k) = 0, \end{aligned} \quad (4)$$

where ε – a small value.

Next, in the system part called “MONITORING SYSTEM OF THE PHASE A,B,C”, the failure symptoms integration procedure for each inverter phase is carried out and then the diagnostic decisions are made. If the transistor fault is localized, the value of the appropriate output signal (T_1 fault, ..., T fault) of the diagnostic system is changed from 0 to 1. In Fig. 7 the block diagram of the monitoring system for the phase A is shown.

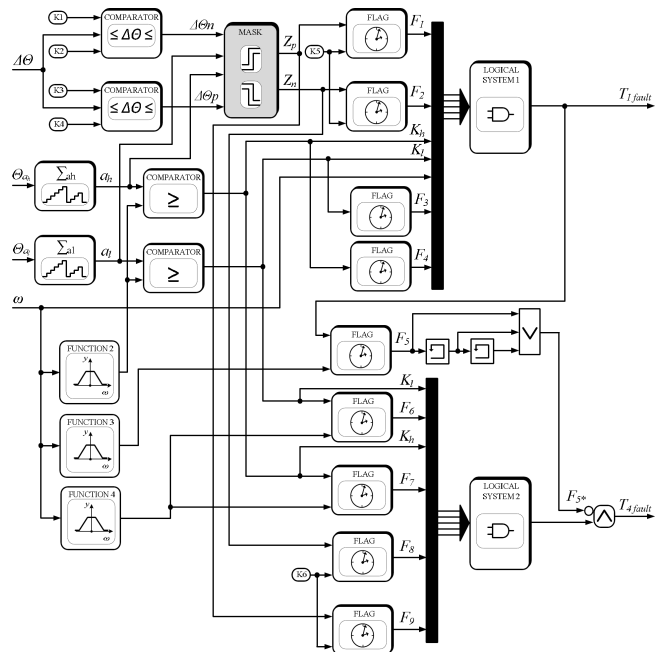


Fig. 7. Monitoring system block diagram of the phase A

The block diagram from Fig. 7 contains two counters: Σ_{ah} and Σ_{al} , which are activated if the value of the Θ_{al} or Θ_{ah} is equal to 1. The number of registered pulses a_h or a_l is

proportional to the time, when the stator current vector takes the characteristic position in the α - β plane (Table 3). If a_h or a_l is equal or bigger than a value appointed by "Function 2" block, the appropriate flag is set for the time dependent on the actual angular motor speed. This flag can be realized as a single bit of a memory space of a microcontroller and it means that some of the previously described characteristic events from Fig. 5, like 1, 3, 4, 6, 7, 9, 10 or 12, was identified. At the same time $\Delta\Theta$ signal is analyzed. If it reaches the value, which is equivalent to the change Θ by π , signal of an appropriate comparator ($\Delta\Theta_n$ or $\Delta\Theta_p$) is set to 1.

The Fig. 7 contains also a block called "MASK", which allows to determine that a sudden change of Θ angle is equal to π and it is simultaneously included between two characteristic positions Θ_{al} and Θ_{ah} . The block diagram of the "MASK" is shown in Fig. 8.

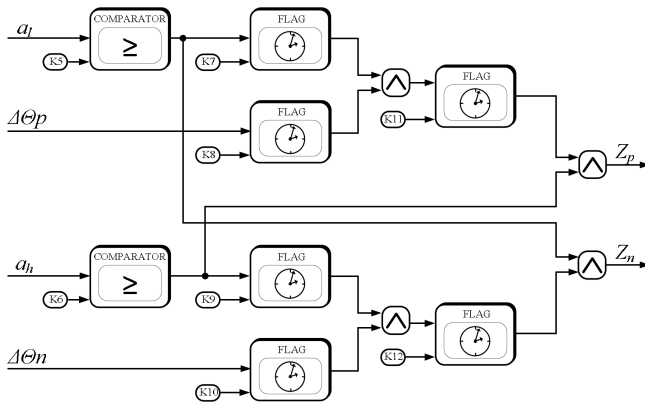


Fig. 8. Block diagram of the "MASK"

It has to be added, that the diagnostic output $T_1 \text{ fault}$ has priority over $T_4 \text{ fault}$. That means, if the fault of the transistor T_1 is localized (if $T_1 \text{ fault} = 1$), a functionality of the logic system which corresponds to the transistor T_4 is deactivated for a while depending on an actual motor speed.

4. Simulation results

To simulate transistor faults, the mathematical model presented in the paper [15] was implemented. According to this model, the phase voltages depend on the phase current and on a healthy semiconductor state in the faulty inverter leg. The transistor failures are simulated by a switch function reconfiguration, so that one directional current flow in the faulty phase is achieved.

The simulation results using the mathematical model of the two-level voltage inverter-fed field-oriented-controlled induction motor drive were obtained (for the induction motor data summarized in the Appendix). The applied speed control structure for the field-oriented control [16, 17] is shown in Fig. 9.

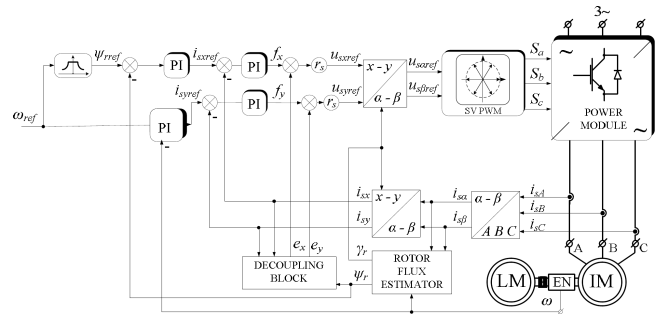


Fig. 9. The adaptive speed control structure for the field-oriented control of induction motor drive

To confirm the correctness of the proposed fault simulation technique, the stator current space vector hodographs under faults of the T_1 - T_6 transistors, for changeable motor speed from the nominal ω_1 up to the low $\omega_4 = 0.25\omega_1$ angular motor speed and constant nominal load torque $m_l = m_n$, are presented in Fig. 10. Their shape and position correspond to ideal vector hodographs presented in Fig. 2.

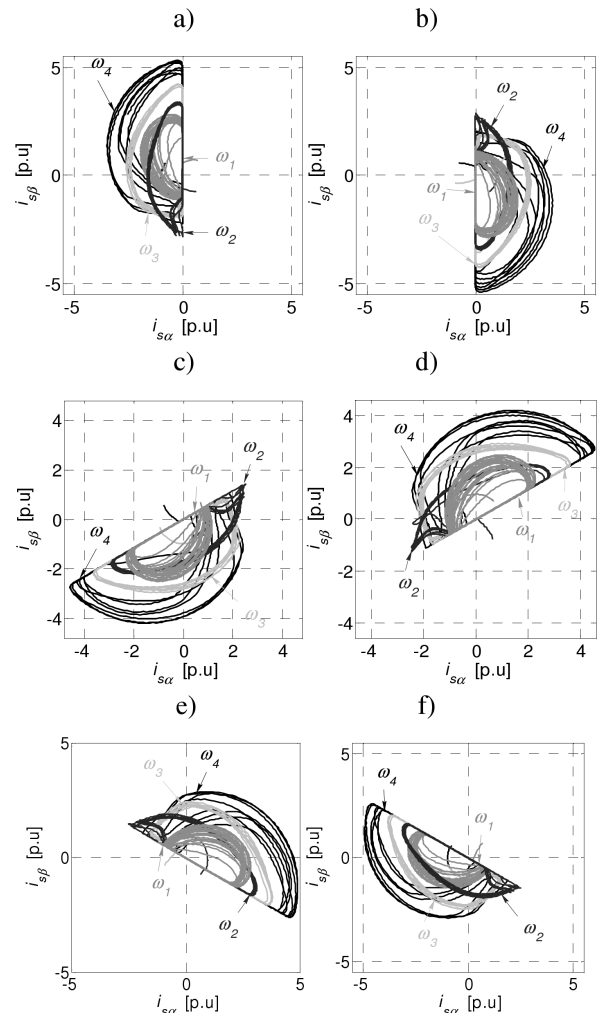


Fig. 10. Hodographs of the stator current space vector during faults of the transistors: T_1 (a), T_4 (b), T_3 (c), T_6 (d), T_5 (e) and T_2 (f) under changeable motor speed $\omega_1 = \omega_n, \dots, \omega_4 = 0.25\omega_n$ and nominal load torque $m_l = m_n$

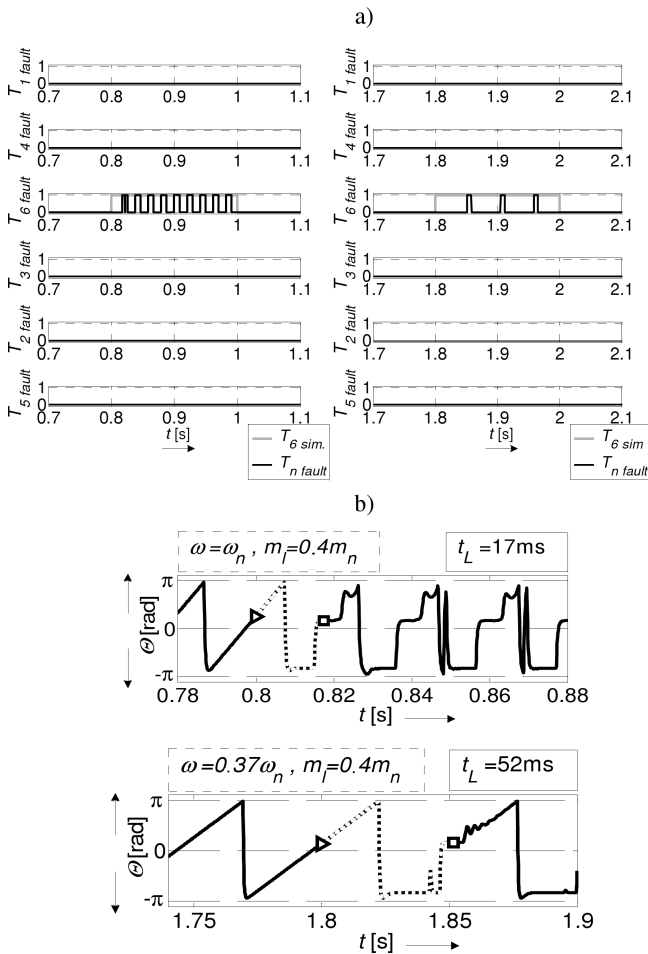


Fig. 11. Output signals of the diagnostic system (a) and Θ signal transients (b) during various positive values of the motor speed ω and constant load torque m_l under steady-state in case of T_6 switch fault

Next the proposed diagnostic method was tested. As the first part of simulation tests, the single open switch faults under speed steady-state operation, for different values and directions of the motor speed ω and load torque m_l are presented. To prove the diagnostic system robustness to false alarms, the $T_1\text{ fault}, \dots, T_6\text{ fault}$ diagnostic signals (Figs. 11a and 12a) under T_6 failure, for both speed directions are presented. Simultaneously the transients of Θ angle signal (Fig. 11b and Fig. 12b) before and during T_6 fault are demonstrated for different speed values. It has to be added, that in the Fig. 11a and Fig. 12a, $T_{6\text{ sim}}$ signal corresponds to a fault simulator. If the failure is simulated, the $T_{6\text{ sim}}$ is equal to one, otherwise – to zero.

In Figs. 11b and 12b the fault occurrence was indicated by triangle, while the rectangle shows a moment when the failure was localized. A part of Θ signal which is referred to a fault localization time t_L is marked by a dotted line.

Figure 13 shows transients of the Θ signal before and during faults of the T_1 - T_6 transistors, for different drive speed values and load condition. In these cases only diagnostic signals corresponding to faulty switches were presented, to illustrate the effectiveness of the proposed diagnostic method.

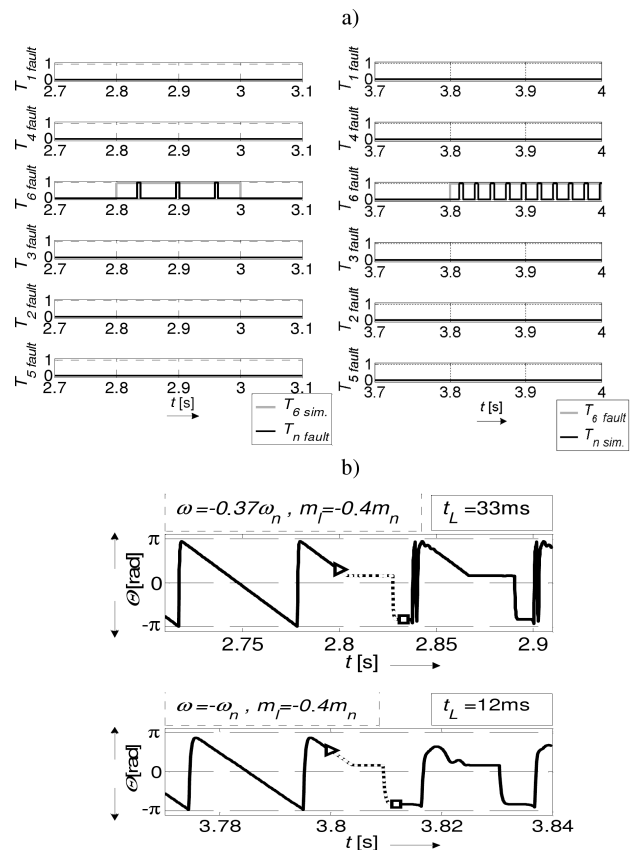


Fig. 12. Output signals of the diagnostic system (a) and Θ signal transients (b) during various negative values of the motor speed ω and constant load torque m_l under steady-state in case of T_6 switch fault

Next, in Fig. 14, simulation results corresponding to faulty inverter condition under dynamical modes – linear speed changes and variable load torque m_l , similar to previously showed examples, are presented.

The simulation results confirm the effectiveness of the proposed diagnostic method under a wide range of the motor drive operating condition. When the current is conducted through the healthy switch of the faulty inverter leg, the Θ angle signal is not affected, so that the failure localization procedure can not be carried out by using the described technique. Accordingly to the diagnostic procedure, the failure symptoms are visible for the diagnostic system when the faulty transistor should to conduct the current. This situation corresponds to the deformed part of the current vector hodographs, which are approximated by the line (diameter of a semicircle – Fig. 2), but taking into account the Θ signal transients, characteristic shapes like in Fig. 5 are registered. As it can be seen in Fig. 10, during low-speed drive operation under transistor fault, the amplitude of stator current vector is significantly higher than in case of nominal speed of the machine. It is related to a relatively long non-current-conducting durations caused by the transistor fault in one of an inverter phase. As a consequence, when a current cannot flow through the transistor, an electromagnetic torque of a machine decreases and therefore in order to maintain its reference value, motor currents are

increased by control circuits in healthy phases. Thus, output signals of drive controllers should be limited so that forced stator currents cannot activate an over-current protection in

case of transistor faults. Fulfillment of this condition allows to effectively perform the proposed transistor fault diagnostic procedure avoiding uncontrolled interrupt of drive operation.

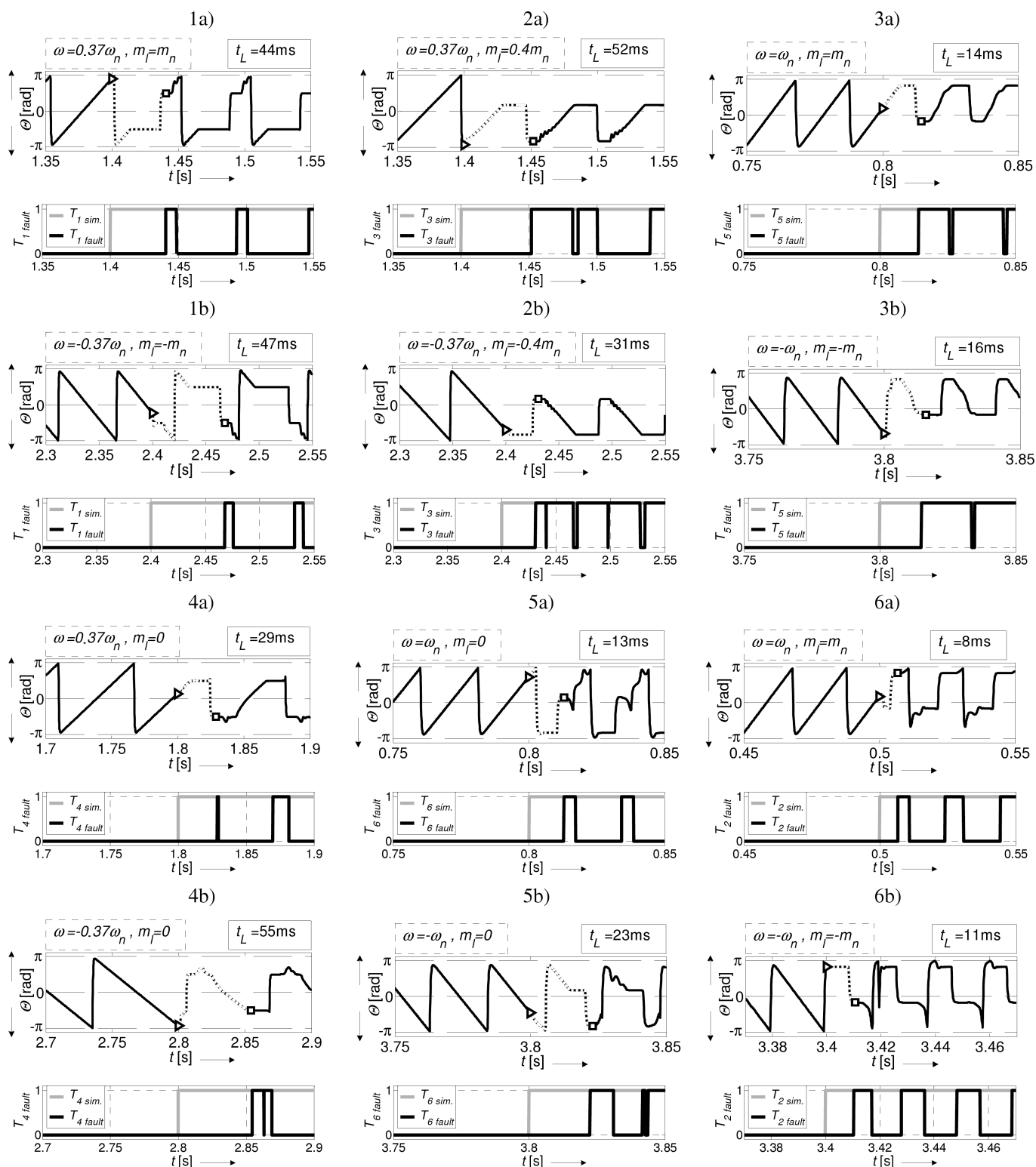


Fig. 13. Output signals of the diagnostic system and the transients of the Θ signal during various angular motor speed ω and a various load torque m_l under steady-state in case of switch fault: T_1 (1a,b), T_3 (2a,b), T_5 (3a,b), T_4 (4a,b), T_6 (5a,b) and T_2 (6a,b)

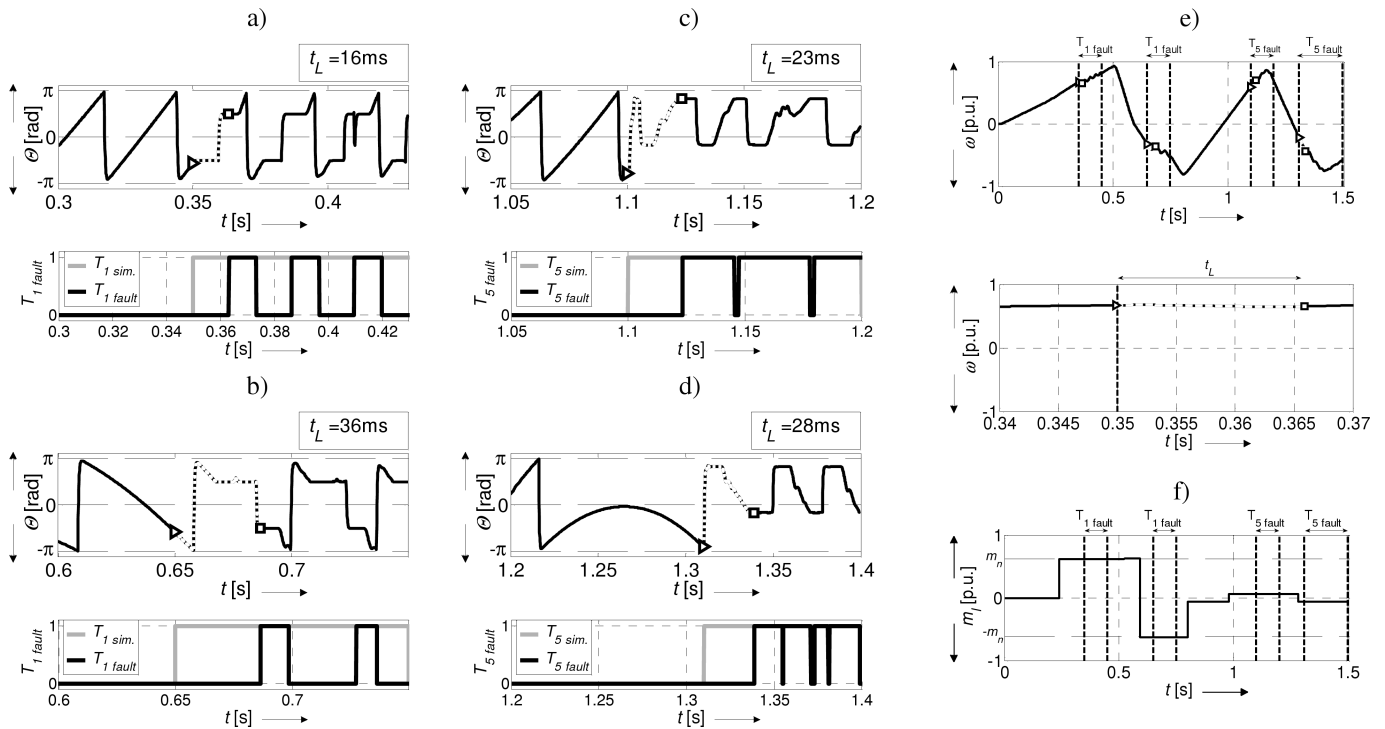


Fig. 14. Transients of the Θ signal during transistor T_1 (a,b) or T_5 (c,d) faults under changeable motor speed ω (e) and a load torque m_1 (f)

The fault localization time t_L depends on an actual position of the current vector in the α - β coordinate system at the moment of the failure occurrence and the angular motor speed as well. According to the proposed diagnostic system, in case of the T_3 , T_4 , T_5 failures, the localization time t_L is always shorter than one period of the stator current, which can be observed in the Figs. 13.2a,b, 13.3a,b, 13.4a,b. However, if the fault of the T_1 , T_2 , T_6 transistors are taken into consideration, t_L can be stretched on and the failure localization procedure is carried out with the time smaller than two current periods. That concerns the situation, when switch fault occurs at the moment referred to the events marked by 2 or 5 in Fig. 5 or during short time periods Δt directly before or after these events. The value of Δt depends on the output signal of the “Function 2” block (Fig. 7) and the velocity of the drive as well. In the proposed diagnostic system, a value of Δt is always shorter than $1/8$ current period, so that the failure localization procedure is carried out during the time t_L which is greater than one stator current period with a probability equal to $1/4$, as can be seen for instance in the Fig. 13.1b.

Simulation results shown in Fig. 14, confirm also the effectiveness of the proposed diagnostic system under dynamical operation of the drive system, e.g. linear changes of the motor speed and various load torque values. Conclusions corresponding to the localization time t_L are analogues as in the case of the switch faults which happen under speed steady-state of the drive, but in this case the current period has to be understood as the time, which is equal to one revolution of the current vector in the α - β coordinate system.

5. Conclusions

The proposed diagnostic system allows to localize the single open-switch faults of the two level voltage inverters under various conditions of the induction motor drive. Due to the introduced adaptation mechanisms of the diagnostic system parameters, the system functionality is not disturbed by so called “false alarms”, even under transient states of the drive speed.

As opposed to the previously mentioned diagnostic methods, for instance the technique based on clustering methods or centroid calculation of the current vector hodographs [8, 9], the proposed diagnostic system implementation does not require large measurement data acquisition and complex calculation as well. The system design is based on simple components such as flip-flops or comparators, therefore the real implementation is relatively cheap and uncomplicated. Thus, the proposed transistor failure diagnostic technique can be applied in fault-tolerant induction motor drive systems that integrate fault diagnostic algorithms and control methods, which always increases computational effort of the control structure.

The analyzed transistor faults contribute to increase inverter phase currents which result in an increased temperature of power modules so that a risk of further faults of power electronics is higher when a faulty motor drive operates for a long term. Nevertheless, as proved in this paper, the proposed diagnostic method provides a short transistor fault localization time which allows to perform a remedial action by utilizing special redundant inverter before occur another failures.

Appendix

Table 4
Three-phase induction motor parameters

Rated power P_N [kW]	1.1
Stator voltage U_N [V]	220/380
Stator current I_N [A]	2.9/5
Speed n_N [rpm]	1400
Number of pole pairs p_p [-]	2
Stator resistance R_s [Ω]	5.90
Stator inductance L_s [H]	0.42
Rotor resistance R_r [Ω]	4.56
Rotor inductance L_r [H]	0.42
Magnetizing inductance L_m [H]	0.39
Inertia of motor drive system J [kgm ²]	0.0142

Acknowledgements. This work was supported by the National Science Centre (Poland) under the project UMO-2013/09/N/ST7/04199.

REFERENCES

- [1] R. Isermann, *Fault-Diagnosis Applications, Model-Based Condition Monitoring: Actuators, Drives, Machinery, Plants, Sensors, and Fault-tolerant Systems*, Springer-Verlag, Berlin, 2011.
- [2] C.T. Kowalski and M. Kaminski, "Rotor fault detector of the converter-fed induction motor based on RBF neural network", *Bull. Pol. Ac.: Tech.* 62 (1), 69–76 (2014).
- [3] S. Yang, D. Xiang, P. Bryant, L. Ran, and P. Tavner, "Condition monitoring for device reliability in power electronic converters: a review", *IEEE Trans. on Power Electronics* 25 (11), 2734–2752 (2010).
- [4] A.M.S. Mendes and A.J. Marques Cardoso, "Voltage source inverter fault diagnosis in variable speed AC drives, by the average current Park's vector approach", *Int. Conf. on Electr. Mach. and Drives* 1, 704–706 (1999).
- [5] R. Peugeot, S. Courtine, and J.-P. Rognon, "Fault detection and isolation on a PWM inverter by knowledge-based model", *IEEE Trans. Ind. Appl.* 34 (6), 1318–1326 (1998).
- [6] W. Sleszynski, J. Nieznanski, and A. Cichowski, "Real-time fault detection and localization vector-controlled induction motor drives", *11th Eur. Conf. on Pow. Electr. and Appl.* 1, 2–8 (2005).
- [7] M. Trabelsi, M. Boussak, and M. Gossa, "Multiple IGBTs open circuit faults diagnosis in voltage source inverter fed induction motor using modified slope method", *19th Int. Conf. on Electr. Mach.* 1, 1–8 (2010).
- [8] Y. Guan, D. Sun, and Y. He, "Mean current vector based on-line real-time fault diagnosis for voltage source inverter fed induction motor drives", *IEEE Electr. Mach. & Drives Conf.* 2, 1114–1118 (2007).
- [9] P. Jang-Hwan, K. Dong-Hwa, K. Sung-Suk Kim, L. Dae-Jong, and C. Myung-Geun, "C-ANFIS based fault diagnosis for voltage-fed PWM motor drive systems", *IEEE Ann. Meet. Fuzzy Inf. Proc.* 1, 379–383 (2004).
- [10] P. Gilreath and B.N. Singh, "A new centroid based fault detection method for 3-phase inverter-fed induction motors", *36th IEEE Pow. Electr. Spec. Conf.* 1, 2664–2669 (2005).
- [11] F. Zidani, D. Diallo, E.H.M. Benbouzid, and R. Nait-Said, "A fuzzy-based approach for the diagnosis of fault modes in a voltage-fed PWM inverter induction motor drive", *IEEE Trans. Ind. Electr.* 55 (2), 586–593 (2008).
- [12] V.F. Pires, T.G. Amaral, D. Sousa, and G.D. Marques, "Fault detection of voltage-source inverter using pattern recognition of the 3D current trajectory", *8th IEEE Reg. Int. Conf. on Comp. Tech.* 1, 617–621 (2010).
- [13] P. Sobanski and T. Orłowska-Kowalska, "Low-cost fault-tolerant control scheme for SVM two-level voltage-inverter-fed induction motor drive with MRASCC speed estimator", *11th Int. Conf. on Modeling and Simul. of Electr. Mach., Converters and Systems Electr. IMACS 2014*, 561–566 (2014).
- [14] T. Orłowska-Kowalska and P. Sobański, "Review of two-level voltage inverters resistant to defect of IGBT transistors", *Scientific Works of the Inst. Electr. Machines., Drives and Measurements of Wrocław Univ. of Technol., ser. Studies and Materials, Ser. Studies and Materials* 33, 54–69 (2013), (in Polish).
- [15] B. Cui, "Simulation of inverter with switch open faults based on switching function", *Proc. IEEE Int. Conf. Automat. and Logist.* 1, 2774–2778 (2007).
- [16] T. Orłowska-Kowalska, *Sensorless Induction Motor Drives*, Wrocław University of Technology Press, Wrocław, 2003.
- [17] G. Extremiana, G. Abad, J. Arza, J. Chivite-Zabalza, and I. Torre, "Rotor flux oriented control of induction machine based drives with compensation for the variation of all machine parameters", *Bull. Pol. Ac.: Tech.* 61 (2), 309–324 (2013).